Journal of Seismology **2:** 37–45, 1998.

Conversion and comparability of data presentations on seismic background noise

P. Bormann
GeoForschungsZentrum Potsdam, Telegrafenberg A17, D-14473 Potsdam, Germany

Received 2 May 1997; accepted in revised form 16 January 1998

Abstract

Data on seismic background noise are collected, amongst others, for assessing the suitability of sites for temporary or permanent seismic recordings. Site quality requirements depend on the task of seismic observations and thus on their resolution, dynamic range, bandwidth and frequency range. Till now noise data are collected with a wide range of instruments, both analog and digital, of different bandwidth, resolution and transfer functions. Accordingly, noise appearence in seismic records, amplitude- and frequency-wise, differs and the various kinds of noise spectra derived therefrom vary too. They are not easily comparable amongst each other and with older presentations of noise 'spectra' derived from analog records. Also, when having determined noise power density spectra from digital records it is not so obvious what this means in terms of noise ground motion amplitudes or noise appearance in records of different bandwidth and vice versa. The paper does not aim at serving as a guide to station site selection but rather to present and comment the relationships to be used for the conversion of power and amplitude spectra into different kinematic units and for calculating from the spectral representations of seismic noise the related frequency dependent RMS or average peak amplitudes of different bandwidth and vice versa. For the new global high (NHNM) and low-noise model (NLNM) given by Peterson (1993) in dB of acceleration power density the related velocity and displacement power spectral densities are presented both graphically and tabulated. Examples for the application of the conversion relationships and the effect of bandwidth on noise and signal amplitudes are given. For a selected data set from a site-selection noise survey in NW Iran the suitability of some potential sites is assessed by comparison with the NLNM.

Introduction

One of the most important steps to be undertaken prior to the selection of suitable seismological recording sites is the investigation of seismic background noise due to artificial (e.g. traffic, machinery) and natural noise sources (e.g. wind, surf, rushing water). Such studies should be carried out in as broad a frequency band as possible, at different potential sites and at different times in order to reveal possible diurnal (mostly man-made) and seasonal (mostly natural) variations. The response curve, resolution and dynamic range of seismographs to be installed at selected recording sites depend both on its noise conditions and the priority task(s) to be performed. Any part of the instrumental dynamic range which falls with more than a few dB within the noise level is useless for seismic signal observations and analysis unless special noise surveys are undertaken in order to reveal the frequency dependent amplification of local subsoil conditions (e.g. Nakamura, 1989; Lachet and Bard, 1994; Field et al., 1995). Consequently, noise studies in connection with site selection surveys are one of the prime tasks of seismological observatory practice (e.g. Bormann et al., 1997).

The Manual of Seismological Observatory Practice (Willmore, 1979) discusses this issue only on the basis of (mostly narrowband) analog recordings and of noise curves derived from visual seismogram inspection and measurement of dominating noise periods and amplitudes. Such noise curves are not comparable with noise spectra determined from nowaday digital recordings, mostly of broadband type. Although the latter are, in a physical and mathematical/quantitative sense, more objective and precise then those derived from the visual inspection of analog records for the station seismolo-

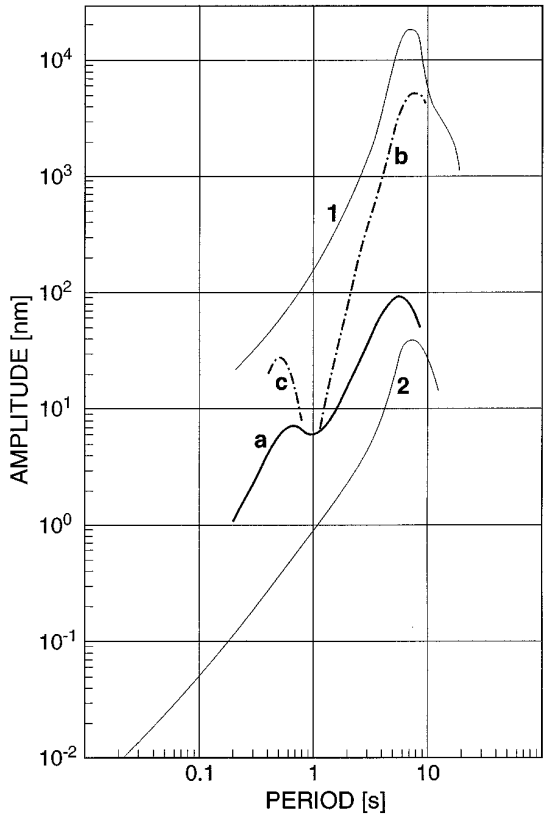

Figure 1. Envelopes of maximum and minimum peak amplitudes for rural environments as determined from analog records of different type over a long time-span according to Brune and Oliver (1959) (curve 1 for high-noise sites and curve 2 for very low-noise sites) together with envelope curves of peak noise amplitudes at station MOX in Germany at times of minimum (curve a) and maximum noise (curves b and c).

gist it is not easily comprehensible what these modern spectral representations mean in terms of ground or recording amplitudes of seismic noise. But the latter determine the frequency-dependent signal-to-noise ratio he is confronted with when analysing seismic records. The IASPEI Commission on Practice decided on its meeting at Wellington in 1994 to establish a special working group entrusted with the elaboration of a new version of the Manual of Seismological Observatory Practice. It should properly reflect the tremendous recent developments, new potentials and requirements in digital seismological practice and try to link the results achieved by means of classical analog and modern digital techniques and procedures. This paper is directly related to this effort.

Noise curves derived from analog recordings

A first compilation of globally published noise data for rural environments as derived from mostly narrow-band analog recordings was made by Brune and Oliver (1959). Disturbances from obvious local noise sources such as nearby traffic or industry, waterfalls, strong winds etc. were not considered. The same applies to any transients of relatively short duration. Accordingly, their envelope curves depicted in Figure 1 represent the maximum and minimum peak amplitudes of seismic noise that might be expected on land in rural environment over a rather long interval of time (about one year).

This first kind of generalized ‘global noise model’ does not consider differences in geological underground conditions nor those in day-time or season. The same applies to the new global model derived from digital data (cf. Figure 2). Accordingly, no real noise spectrum for any given site or period of time will ever precisely follow one of these curves for maximum or minimum noise over the whole period range. Rather there might be situations, where the noise at a far inland continental station being rather near to a major town or industrial center is close to the upper limit for short periods below 1s while the ocean storm microseisms with periods between about 3 to 8 s at this station are close to the minimum curve. On the other hand, a near coastal station but sufficiently far away from man-made short-period noise sources might show the opposite trend. Additionally, the amplitudes of both kinds of noise are not stationary. They show distinct diurnal variations for the man-made noise and seasonal changes in the intensity of ocean storm microseisms. These variations may cover for a given site one to two orders of magnitude in amplitude (and thus two to four orders in power !).

Envelope noise curves which reflect also seasonal and diurnal variations had been determined for the seismological observatory Moxa (MOX), one of the best recording sites in Central Europe. The data were derived from high-frequency (5–50 Hz), short-period (0.5–10 Hz) and KIRNOS broadband recordings (0.05–10 Hz) of that station with magnifications ranging between 1000 and 300 000 times. But limited magnification and recording speed did not allow the measurement of noise amplitudes with $f > 5$ Hz. The respective curves in Figure 1 are envelopes of maximum noise ground amplitudes observed during quietest (a) and noisiest periods of time with b – for seasonal ocean storm microseisms and c – from a near-

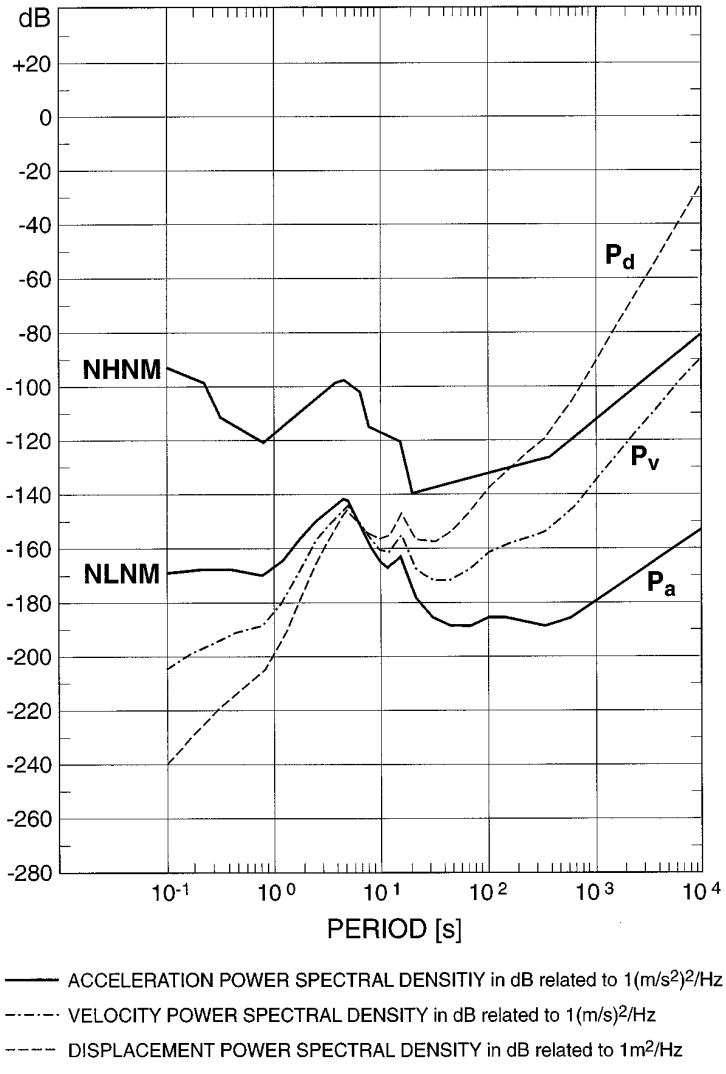

Figure 2. Envelope curves of the new global high (NHNM) and low noise model (NLNM) according to Peterson (1993) in units of dB related to 1 $(m/s^2)^2/Hz$ and the respective curves calculated for the displacement and velocity power spectral density $\mathbf{P_d}$ and $\mathbf{P_v}$ in dB related to 1 $(m/s)^2/Hz$ and 1 m^2/Hz, respectively.

by industrial noise source. The latter produced a pronounced narrowband noise peak around 2 Hz. It was due to the operation of a steel rolling-mill at a distance of about 16 km which has been shut down now. Based on these data an amplitude response curve of a short-period narrowband seismograph was realized by late Ch. Teupser which fitted the combined inverse noise curves b and c. It yielded analog records with peak-to-peak noise trace amplitudes never exceeding 1 mm. They were best suited for detecting weak teleseismic events. This illustrates the advantage of determining such kind of 'noise spectra' by means of visual record inspection and amplitude-period sampling for the optimization of fixed response characteristics of classical seismographs with analog recordings. But one should note that the noise and signal level thus determined depends on the bandwidth of the recording (see 5.).

Noise spectra derived from digital records

Digital seismic records allow proper computational spectral analysis. For a transient signal f(t) the Fourier transform F(ω) exists with

$$F(\omega) = \int_{-\infty}^{\infty} f(t) \exp(i\omega t)\, dt = |F(\omega)| \exp^{i\phi(\omega)} \quad \text{and} \quad (1)$$

$$f(t) = (2\pi)^{-1} \int_{-\infty}^{\infty} F(\omega) \exp(-i\omega t)\, d\omega. \quad (2)$$

|F(ω)| is the *amplitude spectral density* with the unit m/Hz and $\phi(\omega)$ the *phase-delay spectrum* with the units deg, rad or 2πrad. But contrary to *coherent transient seismic signals* f(t) of finite length, as in seismograms from explosions or earthquakes, irradiated by defined localized sources, *ambient seismic noise* is a more or less *stationary stochastic process* without a defined phase-delay spectrum. Therefore, in a strict sense, these two types of signals cannot be measured and compared in the same physical units and thus presented in the same kind of diagram.

A more suitable spectral presentation of seismic noise is the *power spectral density* P(ω). It is the Fourier transform of the autocorrelation function $p(\tau) = \langle f(t)\, f(t+\tau)\rangle$, i.e.

$$P(\omega) = \int_{-\infty}^{\infty} p(\tau) \exp(i\omega\tau)\, d\tau. \quad (3)$$

The symbol $\langle\ \rangle$ indicates averaging over the time t. Depending on whether f(t) is a displacement (d), velocity (v) or acceleration (a) record, P(ω) is given in units m^2/Hz (Figure 4), $(m/s)^2$/Hz or $(m/s^2)^2$/Hz. But when converting displacements $x = a_d \sin\omega t$ into the related velocities dx/dt or accelerations d^2x/dt^2 then one has to consider that the respective velocity and acceleration amplitudes are $a_v = a_d\omega$ and $a_a = a_d\omega^2$, respectively, with $\omega = 2\pi$ f (f – frequency in Hz). Consequently, knowing the displacement power spectral density value $P_d(\omega)$ one can calculate the respective values of the velocity (P_v) or acceleration power spectral density (P_a), i.e.

$$P_v(\omega) = P_d\, \omega^2 = 4\pi^2\, f^2\, P_d \quad (4)$$

and

$$P_a(\omega) = P_d\, \omega^4 = 16\pi^4\, f^4\, P_d = 4\pi^2\, f^2\, P_v \quad (5)$$

or vice versa.

New global noise models according to Peterson

Peterson (1993) published new global high and low noise models. They correspond to the upper and lower bound envelopes of a cumulative compilation of representative ground acceleration power spectral densities (PSD) determined for noisy and quiet periods at 75 world-wide distributed digital stations. These stations were operating under very different environmental conditions, being situated both far inland as well as on islands or near coastal areas. They were placed on a great variety of subsoil/rock types in different distances from urban areas and equipped with seismographs of different bandwidth ranging from short-period to ultra-long period in the range 10^{-2} s to 10^5 s. The data acquisition systems operated with different resolution and sampling rates between 0.01 to 100 s.p.s.. Peterson (1993) carefully screened the records, eliminated seismic events and other transient phenomena, but also times of intense microseismic storms, identified frequency ranges, where instrumental system and/or digitizer noise might dominate the ambient background noise and averaged the spectra of three independent records of quietest and noisiest time periods, respectively. Thus he ensured that his models represent the upper and lower bounds of the *typical* rather than those of the absolute maximum or minimum noise PSD observed. The noise envelopes were approximated by a sequence of straight-line fits and presented in units of dB referred to 1 $(m/s^2)^2$/Hz. with

$$\mathbf{P_a}[\text{dB}] = 10 \log (P_a/1\ (m/s^2)^2/\text{Hz}). \quad (6)$$

Figure 2 shows Peterson's new high- and low-noise models NHNM and NLNM for $\mathbf{P_a}$[dB] together with the NLNM for $\mathbf{P_v}$[dB] and $\mathbf{P_d}$[dB] calculated therefrom by observing the relationships (4), (5) and (6) and the respective units for velocity and displacement power. Substituting in (4) and (5) the frequency f by the period T = 1/f in s we can write:

$$\mathbf{P_v}[\text{dB}] = \mathbf{P_a}[\text{dB}] + 20 \log (T/2\pi) \quad (7)$$

and

$$\mathbf{P_d}[\text{dB}] = \mathbf{P_a}[\text{dB}] + 40 \log (T/2\pi)$$

$$= \mathbf{P_v}[\text{dB}] + 20 \log (T/2\pi). \quad (8)$$

Accordingly, $\mathbf{P_a} = \mathbf{P_v} = \mathbf{P_d}$ for $T = 2\pi = 6.28$ s and $(\mathbf{P_d} - \mathbf{P_a}) = 2 \times (\mathbf{P_v} - \mathbf{P_a}) = $ const. for any given period and negative for $T < 2\pi$ and positive for $T > 2\pi$. Thus, the respective values of $\mathbf{P_d}$ and $\mathbf{P_v}$ for the NHNM can easily be calculated or directly derived from Figure 2.

Table 1. Power spectral densities at selected periods calculated for ground acceleration (P_a), velocity (P_v) and displacement (P_d) according to the new global low-noise model (NLNM) after Peterson (1993)

T [s]	P_a [$m^2\ s^{-4}$/Hz]	$\mathbf{P_a}$ [dB]	P_v [$m^2\ s^{-2}$/Hz]	$\mathbf{P_v}$ [dB]	P_d [m^2/Hz]	$\mathbf{P_d}$[dB]
0.10	1.6×10^{-17}	–168.0	4.1×10^{-21}	–203.9	1.0×10^{-24}	–239.9
0.17	2.1×10^{-17}	–166.7	1.6×10^{-20}	–198.1	1.1×10^{-23}	–229.4
0.40	2.1×10^{-17}	–166.7	8.7×10^{-20}	–190.6	3.5×10^{-22}	–214.6
0.80	1.2×10^{-17}	–169.2	1.9×10^{-19}	–187.1	3.2×10^{-21}	–214.5
1.24	4.3×10^{-17}	–163.7	1.7×10^{-18}	–177.8	6.5×10^{-20}	–191.9
2.40	1.4×10^{-15}	–148.6	2.0×10^{-16}	–157.0	3.0×10^{-17}	–165.3
4.30	7.8×10^{-15}	–141.1	3.6×10^{-15}	–144.4	1.7×10^{-15}	–147.7
5.00	7.8×10^{-15}	–141.1	4.9×10^{-15}	–143.1	3.1×10^{-15}	–145.1
6.00	1.3×10^{-15}	–149.0	1.1×10^{-15}	–149.4	1.0×10^{-15}	–149.8
10.00	4.2×10^{-17}	–163.8	1.0×10^{-16}	–159.7	2.7×10^{-16}	–155.7
12.00	2.4×10^{-17}	–166.2	8.7×10^{-17}	–160.6	3.2×10^{-16}	–155.0
15.60	6.2×10^{-17}	–162.1	3.8×10^{-16}	–154.2	2.3×10^{-15}	–146.3
21.90	1.8×10^{-18}	–177.5	2.2×10^{-17}	–166.7	2.6×10^{-16}	–155.8
31.60	3.2×10^{-19}	–185.0	7.9×10^{-18}	–171.0	2.0×10^{-16}	–156.9
45.00	1.8×10^{-19}	–187.5	9.1×10^{-18}	–170.4	4.7×10^{-16}	–153.3
70.00	1.8×10^{-19}	–187.5	2.2×10^{-17}	–166.6	2.8×10^{-15}	–145.6
101.00	3.2×10^{-19}	–185.0	9.7×10^{-17}	–160.9	2.1×10^{-14}	–136.8
154.00	3.2×10^{-19}	–185.0	1.8×10^{-16}	–157.2	1.1×10^{-13}	–129.4
328.00	1.8×10^{-19}	–187.5	4.9×10^{-16}	–153.1	1.3×10^{-12}	–118.7
600.00	3.5×10^{-19}	–184.4	3.2×10^{-15}	–144.8	3.0×10^{-11}	–105.2
10^4	6.5×10^{-16}	–151.9	3.5×10^{-14}	– 87.9	4.1×10^{-3}	– 23.8
10^5	4.9×10^{-11}	–103.1	1.2×10^{-2}	– 19.1	2.6×10^{6}	+ 65.0

Table 2. Power spectral densities at selected periods calculated for ground acceleration (P_a), velocity (P_v) and displacement (P_d) according to the new global high-noise model (NHNM) after Peterson (1993)

T [s]	P_a [$m^2\ s^{-4}$/Hz]	$\mathbf{P_a}$[dB]	P_v [$m^2\ s^{-2}$/Hz]	$\mathbf{P_v}$[dB]	P_d [m^2/Hz]	$\mathbf{P_d}$[dB]
0.10	7.1×10^{-10}	– 91.5	1.8×10^{-13}	–127.5	4.5×10^{-17}	–163.4
0.22	1.8×10^{-10}	– 97.4	2.2×10^{-13}	–126.5	2.7×10^{-16}	–155.6
0.32	8.9×10^{-12}	–110.5	2.3×10^{-14}	–136.4	6.6×10^{-17}	–162.2
0.80	1.0×10^{-12}	–120.0	1.6×10^{-14}	–137.9	2.6×10^{-16}	–155.8
3.80	1.6×10^{-10}	– 98.0	5.8×10^{-11}	–102.4	2.1×10^{-11}	–106.7
4.60	2.2×10^{-10}	– 96.5	1.2×10^{-10}	– 99.2	6.4×10^{-11}	–101.9
6.30	7.9×10^{-11}	–101.0	8.0×10^{-11}	–101.0	7.9×10^{-11}	–101.0
7.90	4.5×10^{-12}	–113.5	7.1×10^{-12}	–111.5	1.4×10^{-11}	–109.5
15.40	1.0×10^{-12}	–120.0	6.0×10^{-12}	–112.2	3.6×10^{-11}	–104.4
20.00	1.4×10^{-14}	–138.5	1.4×10^{-13}	–128.4	1.4×10^{-12}	–118.4
354.80	2.5×10^{-13}	–126.0	8.0×10^{-10}	– 91.0	2.6×10^{-6}	– 55.9
10^4	9.7×10^{-9}	– 80.1	2.5×10^{-2}	– 16.1	6.2×10^{4}	+ 47.9
10^5	1.4×10^{-5}	– 48.5	3.6×10^{3}	+ 35.5	9.0×10^{11}	+119.6

Tables 1 and 2 give, both in dB and real kinematic units, the corresponding values for the NLNM and NHNM, respectively, for those periods T for which Peterson (1993) gives the line parameters for constructing the models.

From Figure 2 follows that broadband seismometers with an *acceleration* proportional response would need to have a dynamic range of about 100 dB in order to resolve and accommodate without clipping the seismic noise both at quiet and noisy sites in the period

range between 0.1 and 10^3 s. But seismographs with a *velocity* or *displacement* proportional response in that range would require an even larger dynamic range of about 140 dB and 220 dB, respectively. The corresponding figures in the period range between about 1 and 100 s, which is most important for teleseismic recordings, would be about 90 dB, 85 dB and 120 dB for acceleration, velocity and displacement, respectively. Considering only a very low-noise site this is reduced to about 50 dB, 40 dB and 65 dB. Broadband response curves proportional to ground velocity and acceleration are, therefore, best suited for saving a sufficiently large fraction of the dynamic range for signal recording above the noise level. Berckhemer (1971) was the first to hint this in conjunction with his proposed concept of wide band seismometry.

Conversion of spectral amplitude or power densities into recording amplitudes

But how to transform PSD values as in Figures 2 into ground motion amplitudes? According to Aki and Richards (1980) the amplitude of a wavelet f(t) at $t = 0$ can be *roughly approximated* by the product of the amplitude spectral density and bandwidth of the wavelet, i.e.

$$f(t)_{t=0} = |F(\omega)|\ 2\ (f_u - f_l) \tag{9}$$

with f_u and f_l as the upper and lower corner frequencies of the band-passed signal. Likewise, if the power spectral density defined for noise is $P(\omega) = P$ within the frequency band $f_l < f < f_u$ and $P(\omega) = 0$ otherwise, then the *mean square amplitude* is

$$\langle f^2(t)\rangle = 2P\ (f_u - f_l). \tag{10}$$

Thus, for a given bandwidth, we can approximately relate the noise *power spectral density* to its *root mean square* (RMS) amplitude:

$$a_{RMS} = \{2P\ (f_u - f_l)\}^{1/2}. \tag{11}$$

Proper determination and comparability of PSD at different frequencies require octave filtering. Increasing the frequency of a signal by one octave means doubling its frequency. Accordingly, a band-passed signal (or filter) with n octaves of bandwidth has corner frequencies

$$f_u = 2^n\ f_l \tag{12}$$

and *a geometric center frequency* f_o of

$$f_o = (f_u \times f_l)^{1/2} = f_l \times 2^{n/2}. \tag{13}$$

From this follows for the *relative bandwidth* **RBW**

$$(f_u - f_l)/f_o = (2^n - 1)/2^{n/2}. \tag{14}$$

Note: Only when comparing the amplitudes of transient seismic signals and of random noise in a constant relative bandwidth they become commensurable!

Inserting (14) into (11) we get

$$a_{RMS} = (P \times f_o)^{1/2} \times \{2\ (2^n - 1)/2^{n/2}\}^{1/2}$$

$$= (P \times f_o)^{1/2} \times (2\ \mathbf{RBW})^{1/2} \tag{15}$$

Accordingly, the relative bandwith for a 2-octave filter is 1.5 and for a 2/3-octave filter 0.466. Aki and Richards (1980, vol. 1, p. 498) converted PSD into ground motions by putting the bandwidth of the noise signal half the considered (center) frequency, i.e. by assuming $f_u - f_l = 0.5\ f_o$. This is equivalent to the assumption of a bandwidth of approximately 2/3-octaves. For this special case we get:

$$(\langle f^2(t)\rangle)^{1/2} = a_{RMS} = (P \times f_o)^{1/2}. \tag{16}$$

Other authors (e.g. Fix, 1972; Melton, 1978) have used an integration bandwith of 1/3-octave only for computing RMS amplitudes from PSD. Melton reasoned that this is nearly ±10% about the center period in width and thus close to the tolerance with which an analyst can measure the period on an analog seismogram. Therefore, using a 1/3-octave bandwidth seems to be a reasonable convention for calculating RMS noise amplitudes from PSD. The differences as compared to RMS values based on 1/4- or 1/2-octave bandwidths are less than 20%. But 1/3-octave RMS amplitudes will be only about 70% or 50% of the respective RMS amplitudes calculated for 2/3- or 1-octave bandwidth, respectively.

Typical response curves of seismographs have bandwidths of about 1 to 3 octaves for classical narrowband analog recordings (e.g WWSSN short- and long-period seismographs) but 6 to 12 octaves for modern digital broadband instruments. Nevertheless, the signal bandwidth of many dominating and often almost monochromatic components of seismic background noise due to specific noise sources such as ocean storm microseisms with periods around 3 to 7 s or noise from more high-frequent man-made sources are often less than 1 octave (cf. curves for station MOX, Figure 1). Therefore, the above considerations seem to be appropriate.

Contrary to this, transient true ground motion signals from earthquakes and explosions are often rather

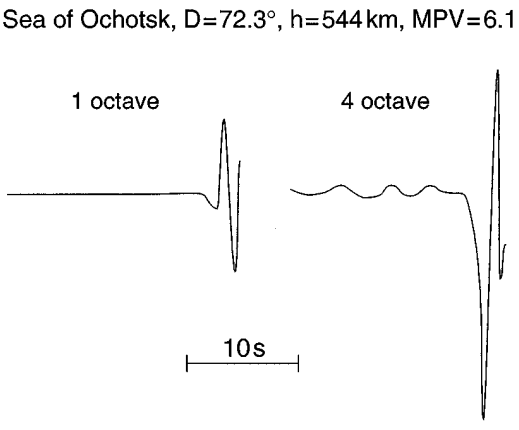

Figure 3. Wavelets of short-period P-wave onsets from a deep earthquake under the Sea of Ochotsk recorded at station MOX, Germany, with identical magnification at 1 Hz but different response characteristics of 1 octave (left) and 4 octaves bandwidth (right).

impulse-like and thus very broadband. When calculating for a given spectral amplitude value of such a transient signal the maximum ground amplitude according to (9) for a much smaller bandwidth then this value is much smaller than that of the true ground motion. This is generally the case with so-called 'true ground motion' amplitudes determined from narrowband recordings of broadband signals by correcting for the amplitude response only. The related magnitude values are accordingly biased.

All considerations above rely on the assumption that eq. (9) is applicable for the considered practical purposes despite of the idealized precondition that $P(\omega) = P$ within the considered frequency band and $P(\omega) = 0$ otherwise. That this nevertheless works sufficiently well is demonstrated by way of example for a seismic signal in Figure 3. Shown are two wavelets of the same P-wave arrival at station MOX from a deep earthquake underneath the Sea of Ochotsk. The true onsets from deep events are rather impulsive and accordingly broadband. But the wave forms shown here differ. They were recorded by two short-period seismographs with identical maximum magnifications at T = 1 s but with different bandwidth of 1 and 4 octaves, respectively. According to (14) their relative bandwidths are then 0.7071 and 3.75 and thus their bandwidth ratio for the same frequency 5.3. The theoretical ratio of the respective maximum amplitudes of bandpassed wavelets with 4- and 1-octave bandwidth as calculated from (9) for identical amplitude spectral density at 1 Hz should then be 2.3. This corresponds precisely to the maximum double-amplitude ratio measured from Figure 3. But the reduction of the first motion amplitude in the 1-octave record is even much larger (about 13 times!) and reveals the generally strong distortion of broadband signals in narrowband records. But when assuming a broad bandpass around the considered spectral frequency then the convertion into ground motion amplitudes means integrating the spectral amplitudes or PSD values over a wide frequency range, thus 'smearing' the frequencies. Accordingly, the more broadband the wavelets the less well defined is their signal period (even becoming aperiodic impulsive) as compared to the more or less monochromatic oscillations of narrowband-filtered signals.

For RMS amplitudes determined according to (11) or (15) there is a 95% probability that the *instantaneous peak* amplitudes of a random wavelet with Gaussian amplitude distribution will lie within a range of $2a_{RMS}$. Peterson (1993) could show, that both broadband and long-period noise amplitudes follow indeed very closely a Gaussian probability distribution. In that case the absolute peak amplitudes of the narrowband filtered signal envelopes should follow closely a Rayleigh distribution. In case of an ideal Rayleigh distribution the theoretical *average peak amplitudes* (APA) are 1.253 a_{RMS}. Peterson (1993) measured from test samples of narrowband filtered VBB and LP noise records APA values between 1.194 and 1.275.

Examples for noise data conversion

We want to test the usefulness of the above relationships for noise conversions. First we convert values of the NHNM into RMS ground motion amplitudes and compare them with the *maximum* noise amplitudes according to curve 1 in Figure 1. For this we use the simple relationship (16) which is based on the assumption of a signal bandwidth of about 2/3 octaves. Taking from Table 2 the values P_d for T = 0.8 s and T = 6.3 s we get for a_{RMS} = 18 nm and 3500 nm, respectively. These values are about 6 times smaller than the respective maximum noise amplitudes over a very long time span according to curve 1 in Figure 1. But according to the above said there is a 5% probability that the instantaneous peak amplitudes are $\geq$ 2 a_{RMS}. If we additionally take into account that Peterson's model represents rather the typical high noise conditions and not the envelop of maximum observed amplitudes as in Brune and Oliver's data (and those for MOX as well!) then both kinds of noise spectra are quantitatively in

RBW = (fu – fl)/fo = (2^n – 1)/(2^(n/2)) (14) f(t)_t=0 = mag(F(w)) 2 (fu – fl) (9)

So 3.75 / 0.7071 = 5.3, this is the bandwidth ratio

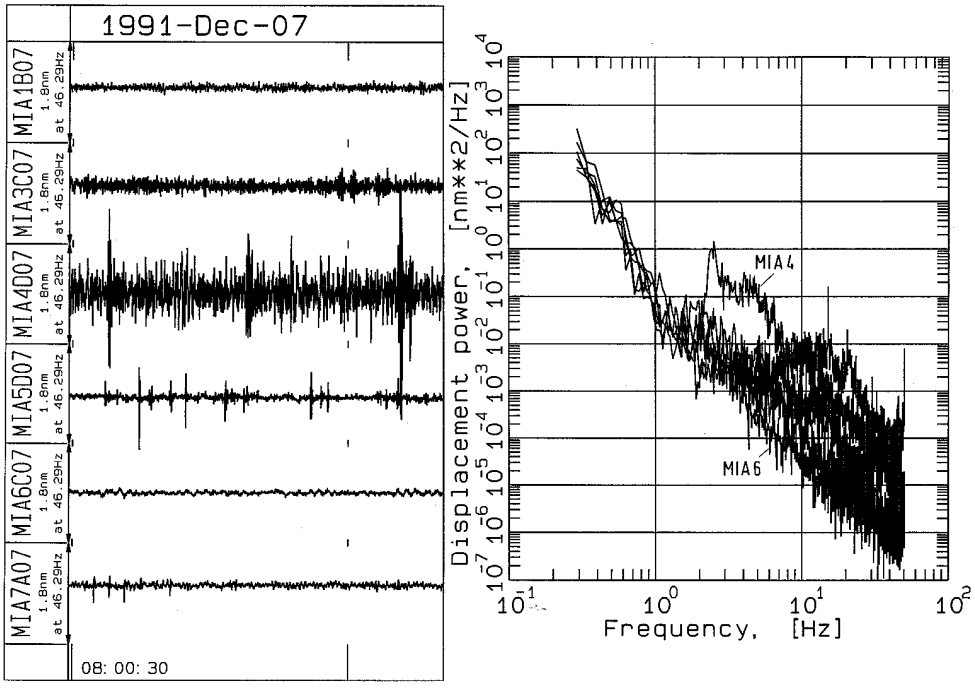

Figure 4. 20s segments of ambient seismic noise recorded at 6 nearby sites in NW Iran about 12 km SW of the town Mianeh (left) and the related displacement power spectral densities (right).

good agreement despite of the great differences in sampling completeness and bandwidth as well as of types of instruments and data analysis used.

Another objective is to compare the noise PSD determined for any given site with that of the global NLNM in order to assess the site quality with respect to background noise conditions. Figure 4 shows several noise record sections together with the respective displacement PSD. They were sampled during a site selection survey in NW Iran. All sites were within about 4 to 12 km SW of the township center of Mianeh. While the recording positions MIA1, 3 and 4 were on unconsolidated Miocene, with MIA4 being additionally on the immediate outskirts of the remote village of Shukhderabad, the positions MIA5-7 were on top of nearby hills of outcropping unweathered andesitic-rhyodacitic rocks. The generally low level of background noise in records of MIA5 was disturbed by high-frequent transients of short duration due to some team members not standing very still within 10 m from the high-resolution sensors. The resulting spectra are, therefore, not representative for this site. The nearby alternative site MIA6 turned out to be the best one sampled in this area. For frequencies 0.3, 1 and 10 Hz the displacement PSD were about 10^{2}, 10^{-1} and 3×10^{-5} nm^2/Hz. Converting these values into units of dB related to 1 m^2/Hz and comparing them with the $\mathbf{P_d}$-curve in Figure 2 we realize that the noise at MIA6 is about 5 dB below (!) the NLNM at f = 0.3 Hz and only about 10 and 15 dB, respectively, above the NLNM for frequencies of 1 and 10 Hz. But at MIA4 next to Shukhderabad, only about 2 km away from MIA6, the noise between f = 2.5 to 5 Hz is already some 35 to 40 dB above the NLNM due to small-scale local village traffic and operating machinery.

Summary

We have discussed the comparability and complementarity of seismic ambient noise spectra determined from analog or digital records for assessing the suitability of recording sites and for selecting the most appropriate recording parameters with respect to seismograph transfer function, bandwidth, resolution and dynamic range. For the new global noise models according to Peterson (1993) the related values for the velocity and displacement power spectral density have been calculated and presented both graphically and in tabulated form. The relationships to convert sig-

nal spectral densities and noise spectral power densities into maximum ground amplitudes or RMS amplitudes and vice versa, have been presented and their usefulness been demonstrated by way of example. Comparing noise data collected in NW Iran during a site-selection field survey for the planned Iranean National Seismic Network with the global noise models it could be shown, that the ambient noise at one of these potential sites was only about 10 dB and 15 dB above the NLNM at f = 1 Hz and 10 Hz, respectively and even 5 dB below the NLNM at f = 0.4 Hz.

Acknowledgements

The data in Figure 4 have been collected in the framework of a UNESCO-sponsored expert mission of the author and Dr Jens Bribach from the GFZ to the Islamic Republic of Iran (Project IRA/90/009) in order to assist the International Institute of Earthquake Engineering and Seismology (IIEES) in Tehran by carrying out seismic noise measurements at potential station sites for the Iranean National Seismic Network (INSN). My sincere thanks go to the Director of the IIEES, Dr Ghafory-Ashtiany, for his kind invitation and the comprehensive technical and logistical support besides boundless hospitality extended to us by the IIEES and its staff members during this mission. He also granted the general permission for the later follow-up detailed data analysis and the publication of results achieved.

I am very much obliged to Dr J. Bribach of the GFZ who joined me as a technical and field expert in this mission, for his unflagging efforts to put the brand new factury-delivered instrumentation into operation, to calibrate its response characteristics, to set the appropriate parameters for the data acquisition system, to manage the data acquisition and handling in the field and to transform the row data into the format required for the later data analysis by using the program SEIS89 written by our colleague Dr Baumbach from the GFZ.

I am also very thankful to Dr H. Grosser from the GFZ for critically reading the manuscript and his useful hints how to improve the clarity of the text and formulae presented and to Prof. E. Wieland for useful comments with respect to the comparison of transient signals and random noise. My gratitute goes also to two anonymous reviewers for their encouraging general support of the paper, some useful hints to a few mistypers and small rounding errors in the tables and for suggesting some more appropriate symbols or less ambigous phrasings in the text.

References

Aki, K. and Richards, P. G., 1980. Quantitative seismology – theory and methods. Vol. 1, W.H.Freeman and Company, San Francisco.

Berckhemer, H., 1971. The concept of wide band seismometry. In: Van Gils, J.-M. (ed.), Proceedings of the XII^{e} Assemblée Générale de la Commission Séismologique Européenne, Luxembourg, 21-29 Septembre 1970, Observatoire Royal de Belgique, Communications, Série A – No. 13, Série Géophysique No. 101, 214–220.

Bormann, P., Wylegalla, K. and Klinge, K.-D., 1997. Analysis of broadband seismic noise at the German Regional Seismic Network and search for improved alternative sites. *J. Seismology* 1: 357–381.

Brune, J. N. and Oliver, J., 1959. The seismic noise of the Earth's surface. *Bull. Seism. Soc. Am.* **49**, 4, 349–353.

Field, E. H., Clement, A. C., Jacob, K. H., Aharonian, V., Hough, S. E., Friberg, P. A., Babaian, T. O., Karapetian, S. S., Hovanessian, S. M. and Abramian, H. A., 1995. Earthquake site-response study in Giumri (formerly Leninakan), Armenia, using ambient noise observations. *Bull. Seism. Soc. Am.* **85**, 1, 349–353.

Fix, J. E., 1972. Ambient Earth motion in the period range from 0.1 to 2560 sec. *Bull. Seism. Soc. Am.* **62**, 1753–1760.

Lachet, C. and Bard, P.-Y., 1994. Numerical and theoretical investigations on the possibilities and limitations of the 'Nakamura's' technique. *J. Physics of the Earth* **42**, 377–397.

Melton, B. S., 1978. The sensitivity and dynamic range of inertial seismographs. *Rev. Geophys. Space Phys.* **14**, 93–116.

Nakamura, Y., 1989. A method for dynamic characteristics estimation of subsurface using microtremor on the ground surface. *Q. Rep. Railway Tech. Res. Inst.* **30**, 1.

Peterson, J., 1993. Observations and modeling of seismic background noise. U.S. Geol. Survey Open-File Report 93-322, 95 pp.